Society for
Mathematical
Biology

ORIGINAL ARTICLE

Check for
updates

Evolution and Adaptation of Anti-predation Response of Prey in a Two-Patchy Environment

Ao Li[1] · Xingfu Zou[1]

Abstract

When perceiving a risk from predators, a prey may respond by reducing its reproduction and decreasing or increasing (depending on the species) its mobility. We formulate a patch model to investigate the aforementioned fear effect which is indirect, in contrast to the predation as a direct effect, of the predator on the prey population. We consider not only cost but also benefit of anti-predation response of the prey, and explore their trade-offs together as well as the impact of the fear effect mediated dispersals of the prey. In the case of constant response level, if there is no dispersal and for some given response functions, the model indicates the existence of an evolutionary stable strategy which is also a convergence stable strategy for the response level; and if there is dispersal, the analysis of the model shows that it will enhance the co-persistence of the prey on both patches. Considering the trait as another variable, we continue to study the evolution of anti-predation strategy for the model with dispersal, which leads to a three-dimensional system of ordinary differential equations. We perform some numerical simulations, which demonstrate global convergence to a positive equilibrium with the response level evolving towards a positive constant level, implying the existence of an optimal anti-predation response level.

Keywords Predator–prey system · Fear effect · Adaptive dynamics · Evolution · Patchy environment · Dispersal

✉ Xingfu Zou
  xzou@uwo.ca

  Ao Li
  ali297@uwo.ca

[1] Department of Applied Mathematics, University of Western Ontario, London, ON N6A 5B7, Canada

Springer

1 Introduction

Interactions between predator and prey species are typically very complicated, in comparison with competitions and mutualism. This is mainly because a dynamical system model that describes predator–prey interaction is non-monotone, and hence, can allow very rich dynamics.

The most classic predator–prey system was proposed by Lotka and Volterra, respectively, in 1920s, and is of the following form:

$$
\begin{cases}
\dfrac{du}{dt} = \alpha u - \beta uv, \\
\dfrac{dv}{dt} = -\delta v + \gamma uv,
\end{cases}
\tag{1}
$$

where $u(t)$ and $v(t)$ are the populations of the prey and predator, respectively, at time t. This model allows a family of periodic orbits and is structurally unstable. Since then, there have been numerous modifications/generalizations on (1), which can be represented by the following more general form:

$$
\begin{cases}
\dfrac{du}{dt} = g_1(u) - p(u, v)v, \\
\dfrac{dv}{dt} = g_2(v) + cp(u, v)v,
\end{cases}
\tag{2}
$$

where $g_1(u)$ ($g_2(v)$) represents the population dynamics of the prey (predator) in the absence of the predator (prey). Here the predation term $p(u, v)v$ accounts for catching/consumption rate of prey by predator, and is a *direct effect* of the predator on prey. The positive constant c explains the efficiency of biomass transfer from prey to predator after catching and consumption, and the function $p(u, v)$ is referred to as the functional response. To the authors' knowledge, almost all efforts in modifying and generalizing (1) lie in proposing various forms for $p(u, v)$ depending on the nature of predation which is species specific. For example, for $p(u, v)$ depending on u only, there are Holling types I, II and III; for $p(u, v)$ truly depending on both u and v, there are Beddington–DeAngelis functional response $p(u, v) = \frac{au}{1+bu+cv}$ and ratio-dependent functional response $p(u, v) = \frac{a(u/v)}{c+b(u/v)} = \frac{au}{bu+cv}$. Therefore, such efforts are all along the line of the *direct effect*.

On the other hand, recent field observations and empirical results show that merely the presence of predator can alter ecological behaviours of prey, and thereby, influence its population size. For feeding animals, they may change their foraging periods and locations to avoid hunting predators (Lima and Dill 1990). Such effects are *indirect* and non-lethal as they are not through predation and consumption. Usually, defensive actions, including avoidance, vigilance, alarm calls, grouping and even defences against predators (Cresswell 2008) can diminish direct mortality from predation temporally, but will decrease lifetime fitness as well through, for example, reduced growth rate and fecundity due to less intake and mating opportunities.

To study how significant such a fear effect can be, some experiments have been designed and conducted by limiting lethal consumption. For example, Nelson et al. (2004) surgically shortened the mouthparts of damsel bugs, so that they were unable to consume pea aphids but could still disturb them. The growth of aphid population was reduced by 30%. Zanette et al. (2011) conducted a field experiment on song sparrows. They protected the birds from direct predation by using electric fences and broadcasted playbacks of the calls and sounds of their predators. They found that number of the bird's offspring per year was reduced by 40%. Preisser et al. (2005) estimated the sizes of direct and indirect effects in 166 studies from 49 published works, and their result showed that the indirect effect size on average was similar to (more precisely it was only slightly weaker than) the direct effect size.

The aforementioned field experimental results clearly indicate that fear effect is indeed an important factor in predator–prey interactions. As far as mathematically modelling fear effect is concerned (Brown et al. 1998) firstly modelled the ecology of fear by conjoining the Rosenzweig–MacArthur model (Rosenzweig and MacArthur 1963):

$$
\begin{cases}
\dfrac{du}{dt} = ru\left(1 - \dfrac{u}{K}\right) - g(u)v, \\
\dfrac{dv}{dt} = -mv + eg(u)v,
\end{cases}
\tag{3}
$$

with a foraging theory in 1999, where fear was represented by the level of vigilance. In a recent work, based on the field study in Zanette et al. (2011), Wang et al. (2016) incorporated the fear effect on reducing the reproduction rate of the prey in the Rosenzweig–MacArthur model with Holling types I and II functional responses. In Wang and Zou (2017), Wang and Zou further discussed different effects of fear on juvenile and adult stages of the prey by a model with age structure, in the form of a system of delayed differential equations. Note that in Wang et al. (2016), only a cost of the anti-predation response was considered. More recently, Wang and Zou (2020) modified the model in Wang et al. (2016) by (i) incorporating both cost (reducing reproduction rate) and benefit (reducing the chances of being caught and consumed by predator) to the prey equation and (ii) introducing a time lag that accounts for the time needed for the transfer of prey biomass to predator biomass. The analysis in Wang and Zou (2020) has not only shown that there is a critical response level, but also revealed how such a critical level is affected by the digestion delay. Sasmal and Takeuchi (2020) also considered both cost and benefit due to anti-predation response with the functional response $g(u)$ being Holling type IV, and explored the rich dynamics of the resulting ODE system. Sasmal (2018) explored multiple Allee effect induced by fear effect. From the aforementioned works, it seems that the fear effect had been largely neglected in predator–prey models, and the recent results mentioned above suggest that many existing models deserve a revisit by incorporating the fear effect and various factors induced by such an indirect effect in predator–prey interactions.

Besides the factors mentioned above (age structure, types of the functional responses, digestion delay), there is also the important factor of spatial structure. Considering the ability of species moving around, many works have already been

done for both *discrete* and *continuum* habitats by using random dispersal or diffusion to model the movement of individuals [for example, see Hastings (1982), Levin et al. (1984), Jansen (2001), Okubo and Levin (2001) and the references therein]. In most existing works, dispersal rates were postulated to be constants, independent of time, location and population densities. However, in predator–prey interactions, some prey perceiving a predation risk from the predator may accordingly change their dispersal strategy to avoid encounters with predators. In most cases, animals (such as mice) are observed to reduce their activities because moving prey is more likely to be detected by predators; usually, this corresponds to the increased use of refuges (Lima and Dill 1990). There are also biological species, such as birds which, upon perceiving a risk from the predators, in addition to reducing the reproduction rate, may respond to the risk by moving more frequently and in more advantageous direction(s). For a spatially *continuum* habitat, Wang and Zou (2018) proposed and analysed a reaction–diffusion model with predator-taxis for the prey accounting for the prey's intention of moving away from the predator. Through the model, the role of fear effect in pattern formation is explored in conjunction with various types of functional responses.

Compared to partial differential equation models for populations in a spatially continuous habitat, patch models for discrete habitats are sometimes more practical since habitat fragmentation is common. For human beings, we live in cities and towns; for animals, the land is often separated by geographical factors and human constructions. With the above considerations, it is interesting and desirable to explore how the fear effect reflected not only in reproduction rate but also in dispersal rate of the prey will affect the population dynamics in predator–prey interactions. To this end, parallel to Wang and Zou (2018), we propose in this work a predator–prey model in the form of system of ordinary differential equations over two patches. In Sect. 2, we will formulate and explain our model; and in subsequent Sects. 3 and 4, we will analyse the model to gain some biological insights into the role of fear effect in conjunction with the dispersals. We begin in Sect. 3 by considering the case without dispersal; this will allow us to obtain some preliminary results on the fear effect on local population dynamics and the evolution of anti-predation response level. Then, in Sect. 4, we further explore the case when the two patches are connected through dispersals with dispersal rates also affected by fear. Some numerical simulations are presented. We complete the paper by Sect. 5, summarizing the main results and discussing the biological implications and significance of the results, as well as some possible related future research projects.

2 Model Formulation

The logistic growth of prey population in the Rosenzweig–MacArthur model (3) is a result of constant per capita birth rate b_0 together with a density independent per capita death rate (nature death rate) d_1 and a density-dependent death rate d_2u: $u'(t) = b_0u - d_1u - (d_2u)u = (b_0 - d_1)u[1 - \frac{u}{(b_0-d_1)/d_2}]$. Based on this and the field experiment of Zanette et al. (2011) where predation was artificially prevented, Wang et al. (2016) proposed the following predator–prey model:

$$\begin{cases} \dfrac{du}{dt} = b_0 f(\alpha, v)u - d_1 u - d_2 u^2 - g(u)v, \\ \dfrac{dv}{dt} = -mu + cg(u)v, \end{cases} \tag{4}$$

where a specialist predator was considered and Holling types I and II for the functional response function $g(u)$ were adopted in respective analysis. Here, v denotes the population of predators reflecting the level of risk, and α is a non-negative parameter reflecting the anti-predation response level of the prey and hence, the decreasing properties of $f(\alpha, v)$ in α and v posed in Wang et al. (2016) account for the effect of the prey's fear on reducing the prey's reproduction rate.

Note that the demographic equation in (4) for the prey population assumes a constant per capita birth rate, which has neglected the Allee effect for the prey species. Allee effect reflects the fact that for some two-sex species, the per capita birth rate is also density dependent due to the need in group defence and/or mating opportunities. A simple dependence is $b(u) = b_0 + b_1 u$, reflecting the scenario that larger the population size is, more mating opportunities there will be and hence, more births there will be. This simple $b(u)$ will also lead to a logistic growth for the prey in the absence of the predator, with the carrying capacity modified accordingly. There has been many research on modelling Allee effect using various density-dependent birth rate functions; see Terry (2015) and the references therein for more details on this topic. We also point out that there are also two-sex species for which a matured individual only mates with a fixed partner. Considering this fact and in order to avoid making things too complicated, we will not consider Allee effect but just follow the line of (4).

With the same consideration for the prey population as in (4), we consider a prey species that lives on two patches and is able to move between the two patches. Let u_i and v_i denote the populations of prey and predators on patch i ($i = 1, 2$), respectively. We then propose the following model system:

$$\begin{cases} \dfrac{du_1}{dt} = b_1(\alpha, v_1)u_1 - d_1 u_1 - au_1^2 - c(\alpha, v_1)u_1 v_1 + m(\alpha, v_2)u_2 - m(\alpha, v_1)u_1, \\ \dfrac{du_2}{dt} = b_2(\alpha, v_2)u_2 - d_2 u_2 - au_2^2 - c(\alpha, v_2)u_2 v_2 + m(\alpha, v_1)u_1 - m(\alpha, v_2)u_2. \end{cases} \tag{5}$$

Here, the Holling type I functional response is adopted for predation interactions, and the birth rate functions $b_i(\alpha, v_i)$, predation rate functions $c(\alpha, v_i)$ and dispersal rate functions $m(\alpha, v_i)$ are assumed to depend on the perceived predation risk (represented by the quantity of predators v_i) and vigilance level $\alpha \in (0, \infty)$ (considered as an anti-predation strategy) of the prey, for $i = 1, 2$. We allow *spatial heterogeneity* in the two patches in resources and this leads to the adoption of patch specific birth rate functions. On the other hand, considering that we are dealing with the *same prey species* living in two different patches *predated by the same predator species*, we have assumed the same predation rate function and dispersal rate function in the two patches, both depending on predator population in the patch though. In order to focus on the prey's

population and for simplicity, we assume that the predator has a constant population on each patch, meaning that v_1 and v_2 are positive constants. This approximately corresponds to a scenario that the predator is a generalist species living on a wide range of food resources and only having this prey species as a minor food resource.

According to the discussion in the introduction, prey reduce reproduction in response to the perceived predation risk, and being more alert gives them higher chances to survive through predation. To capture these biological meanings, functions $b_i(\alpha, v_i)$ and $c(\alpha, v_i)$ are assumed to satisfy the following properties which are similar to those in Wang et al. (2016):

$$
\begin{cases}
b_i(0, v_i) = b_i(\alpha, 0) = b_{0i}, \\
\lim_{\alpha \to \infty} b_i(\alpha, v_i) = \lim_{v_i \to \infty} b_i(\alpha, v_i) = 0, \\
c(0, v_i) = c(\alpha, 0) = c_0, \\
\lim_{\alpha \to \infty} c(\alpha, v_i) = \lim_{v_i \to \infty} c(\alpha, v_i) = 0, \qquad i = 1, 2. \\
\dfrac{\partial b_i(\alpha, v_i)}{\partial \alpha} \le 0, \quad \dfrac{\partial b_i(\alpha, v_i)}{\partial v_i} \le 0, \\
\dfrac{\partial c(\alpha, v_i)}{\partial \alpha} \le 0, \quad \dfrac{\partial c(\alpha, v_i)}{\partial v_i} \le 0,
\end{cases}
\tag{6}
$$

In Wang et al. (2016), the authors presented three examples of such function satisfying the above conditions:

$$
h_1(\alpha, v) = a_1 e^{-b_1 \alpha v}, \quad h_2(\alpha, v) = \frac{a_2}{1 + b_2 \alpha v} \quad \text{and}
$$

$$
h_3(\alpha, v) = \frac{a_3}{1 + b_3 \alpha v + c_3 (\alpha v)^2}.
$$

As for the dispersal rate function $m(\alpha, v_i)$, it is species specific: when perceiving predation risk, some species may tend to move more frequently (e.g., birds), while the others may reduce their movement to avoid being captured (e.g., mice which typically have refuges). We consider the latter in this work by assuming that the dispersal rate function is decreasing with respect to α and v_i:

$$
\begin{cases}
m(0, v_i) = m(\alpha, 0) = m_0, \quad \lim_{\alpha \to \infty} m(\alpha, v_i) = \lim_{v_i \to \infty} m(\alpha, v_i) = 0, \\
\dfrac{\partial m(\alpha, v_i)}{\partial \alpha} \le 0, \quad \dfrac{\partial m(\alpha, v_i)}{\partial v_i} \le 0.
\end{cases}
\tag{7}
$$

Let $F_i(\alpha, v_i) = b_i(\alpha, v_i) - d_i - c(\alpha, v_i)v_i$ for $i = 1, 2$. Note that $F_i(\alpha, v_i)$ can be used as a measure of fitness for the species on patch i. Then, the model (5) is rewritten as:

$$
\begin{cases}
\dfrac{du_1}{dt} = u_1 [F_1(\alpha, v_1) - au_1] + m(\alpha, v_2)u_2 - m(\alpha, v_1)u_1, \\
\dfrac{du_2}{dt} = u_2 [F_2(\alpha, v_2) - au_2] + m(\alpha, v_1)u_1 - m(\alpha, v_2)u_2.
\end{cases}
\tag{8}
$$

According to the basic theory of ordinary differential equations, there exists a unique solution to system (8) for any given initial values $u_1(0)$ and $u_2(0)$. Using the proposition given by Chepyzhov and Vishik in their book (Chepyzhov and Vishik 2002, Proposition 1.1), one can easily check that $\mathbb{R}^2_+$ is invariant for (8). Moreover, setting $\bar{F} = \max\{F_1(\alpha, v_1), F_2(\alpha, v_2) : \alpha \geq 0, v_1 \geq 0, v_2 \geq 0\}$, we have

$$\frac{d}{dt}(u_1 + u_2) \leq (u_1 + u_2)\left[\bar{F} - \frac{a}{2}(u_1 + u_2)\right].$$

By a comparison argument, we then conclude that

$$\limsup_{t \to \infty}(u_1 + u_2) \leq \frac{2\bar{F}}{a},$$

indicating that the total population $(u_1 + u_2)$ is bounded. By the non-negativity of u_1 and u_2, both of them must be bounded. Furthermore, if $\bar{F}$ is non-positive, then the total population $(u_1 + u_2)$ converges to zero.

Summarizing the above, we have obtained the following result of well-posedness for the model.

Lemma 2.1 *For any initial point $[u_1(0), u_2(0)] \in \mathbb{R}^2_+$, there exists a unique solution to system (8) which is non-negative and bounded.*

3 Model Analysis: Without Dispersal

We begin our analysis of the model for local population dynamics by considering the case *without dispersal: $m(\alpha, v_1) = m(\alpha, v_2) = 0$*. Then, the model (8) reduces to a decoupled pair of ordinary differential equations (ODEs) with each having the same form of

$$\frac{du}{dt} = u\left[F(\alpha, v) - au\right], \tag{9}$$

where $F(\alpha, v) := b(\alpha, v) - d - c(\alpha, v)v$. This is a scalar logistic ODE in terms of the variable u and its dynamics is completely well known:

Lemma 3.1 *If $F(\alpha, v) \leq 0$, then every solution of (9) with $u(0) \geq 0$ converges to 0; if $F(\alpha, v) > 0$, then every solution of (9) with $u(0) > 0$ satisfies*

$$\lim_{t \to \infty} u(t) = \frac{F(\alpha, v)}{a}.$$

Before moving on to the patch model *with dispersal*, we want to gain some insights into the anti-predation strategy of prey from evolutionary perspective by using the method of adaptive dynamics. To this end, we take the vigilance level parameter α as the trait. Assume that a resident prey with population size u uses the strategy α_u and a mutant (or invading) prey with relatively small population size w ($w \ll u$) adopts

a different strategy $\alpha_w \neq \alpha_u$, and the resident and mutant strains are ecologically equivalent in all other aspects. Then, model (9) is naturally extended to the following system of equations:

$$
\begin{cases}
\dfrac{du}{dt} = u[F(\alpha_u, v) - a(u+w)] =: g^u(u, w), \\
\dfrac{dw}{dt} = w[F(\alpha_w, v) - a(u+w)] =: g^w(u, w).
\end{cases}
\tag{10}
$$

Suppose that the population of resident prey has already settled at the steady state $u^*(\alpha_u, v) = \frac{F(\alpha_u, v)}{a} =: P(\alpha_u, v)$ (assuming $F(\alpha_u, v) > 0$) if there is no invading (mutant) prey competing with it. The idea of invasibility analysis (see Diekmann 2004 for more details) is to find out whether the population of mutant prey will grow or decay once introduced. This corresponds to the local instability/stability of the boundary equilibrium $(P(\alpha_u, v), 0)$ of (10). Notice that (10) is a Lotka–Volterra competition model with the equal competition weight, and hence, the competition exclusion is the generic consequence in the following sense:

(i) if $F(\alpha_w, v) > F(\alpha_u, v)$, then equilibrium $E_w := (0, P(\alpha_w, v))$ is globally asymptotically stable for (10);

(ii) if $F(\alpha_w, v) < F(\alpha_u, v)$, then equilibrium $E_u := (P(\alpha_u, v), 0)$ is globally asymptotically stable for (10).

Following Diekmann (2004), we introduce the invasion exponent $\theta(\alpha_u, \alpha_w)$ for the mutant prey by

$$
\theta(\alpha_u, \alpha_w) = \left.\frac{\partial g^w(u, w)}{\partial w}\right|_{w=0} = F(\alpha_w, v) - au^*(\alpha_u, v) = F(\alpha_w, v) - F(\alpha_u, v),
$$

which is the relative fitness of the mutant in the environmental condition mediated by the residents. Then, the above competition exclusion results can be restated in terms of the sign of this invasion exponent $\theta(\alpha_u, \alpha_w)$: the mutant prey will invade and replace the resident prey if $\theta(\alpha_u, \alpha_w) > 0$; and the mutant prey cannot invade (establish) if $\theta(\alpha_u, \alpha_w) < 0$.

Next, we explore the existence of evolutionary stable strategy (ESS) and convergence stable strategy (CSS) with respect to the fitness function $F(\alpha, v)$. An evolutionary singular strategy $\alpha_u = \alpha^*$ is a trait value at which the selection gradient vanishes,

$$
\left.\frac{\partial \theta(\alpha_u, \alpha_w)}{\partial \alpha_w}\right|_{\alpha_w = \alpha_u} = \left.\frac{\partial F(\alpha_w, v)}{\partial \alpha_w}\right|_{\alpha_w = \alpha^*} = 0.
\tag{11}
$$

If the resident prey using strategy α^* cannot be invaded by any mutant prey using other strategies, then α^* is an ESS. By Day and Burns (2003) and Diekmann (2004), this is implied by

$$
\left.\frac{\partial^2 \theta(\alpha_u, \alpha_w)}{\partial \alpha_w^2}\right|_{\alpha_w = \alpha_u = \alpha^*} = \left.\frac{\partial^2 F(\alpha_w, v)}{\partial \alpha_w^2}\right|_{\alpha_w = \alpha^*} < 0.
\tag{12}
$$

The singular point α^* is a CSS if among any pair of strategies near α^*, the one closer to α^* is always the winning strategy. By Day and Burns (2003) and Diekmann (2004), this is implied by

$$\frac{d}{d\alpha_u}\left[\left.\frac{\partial\theta(\alpha_u,\alpha_w)}{\partial\alpha_w}\right|_{\alpha_w=\alpha_u}\right]_{\alpha_u=\alpha^*} = \left.\frac{\partial^2 F(\alpha_w,v)}{\partial\alpha_w^2}\right|_{\alpha_w=\alpha^*} < 0. \tag{13}$$

By condition (12), a local maximum of function $F(\alpha_w,v)$ is a local ESS. Moreover, conditions (12) and (13) are equivalent for model (10), implying that the ESS must be convergence stable when exists.

For a general discussion on definition and biological meanings of ESS and CSS, readers are referred to Diekmann (2004) and Geritz et al. (1998). Here in this paper, the abbreviation CSS is used to denote a convergence stable strategy, but in some works, it denotes a continuously stable strategy, which is by definition a convergence stable ESS. For convenience of associating the notions of ESS and CSS with the stability/instability, we adopt the definitions of ESS and CSS used by De Leenheer et al. (2017) for a setting without dispersal as below.

Definition 3.1 (*Definition 3.1 in* De Leenheer et al. 2017) The anti-predation strategy $\alpha^* \in [0,\infty)$ is an ESS if the boundary equilibrium $(u^*(\alpha^*,v),0)$ of system (10) is locally asymptotically stable for all $\alpha_w \neq \alpha^*$ in some neighbourhood of α^*.

Definition 3.2 (*Definition 3.2 in* De Leenheer et al. 2017) The anti-predation strategy $\alpha^* \in [0,\infty)$ is a CSS if there is a neighbourhood N of α^* such that the boundary equilibrium $(u^*(\alpha_u,v),0)$ of system (10) is locally asymptotically stable for all $\alpha_u,\alpha_w \in N$ that satisfy $\alpha_w < \alpha_u < \alpha^*$ or $\alpha_w > \alpha_u > \alpha^*$ but is not locally asymptotically stable when $\alpha_u < \alpha_w < \alpha^*$ or $\alpha_u > \alpha_w > \alpha^*$.

To proceed further to explore the possible ESS and CSS, we choose some particular forms for the functions $b(\alpha,v)$ and $c(\alpha,v)$ as below:

$$b(\alpha,v) = b_0 e^{-\tilde{s}\alpha v}; \quad c(\alpha,v) = c_0 e^{-\tilde{p}\alpha v}. \tag{14}$$

Absorbing the positive constant v by letting $s = \tilde{s}v$ and $p = \tilde{p}v$, the fitness function $F(\alpha,v)$ is a single variable function,

$$F(\alpha,v) = F(\alpha) = b_0 e^{-s\alpha} - d - c_0 v e^{-p\alpha}. \tag{15}$$

Analysis on $F(\alpha)$ distinguishes two cases: (i) $p > s$; and (ii) $p < s$, with their respective consequences summarized below.

(i) Assume $p/s > 1$, then

    (i)-1 if $\frac{p}{s} < \frac{b_0}{c_0 v}$, then $F'(\alpha) < 0$ for all $\alpha > 0$ and there is no critical point for $F(\alpha)$;

    (i)-2 if $\frac{p}{s} > \frac{b_0}{c_0 v}$, then $F(\alpha)$ has a unique critical point $\alpha^* > 0$ at which $F(\alpha)$ attains a maximum;
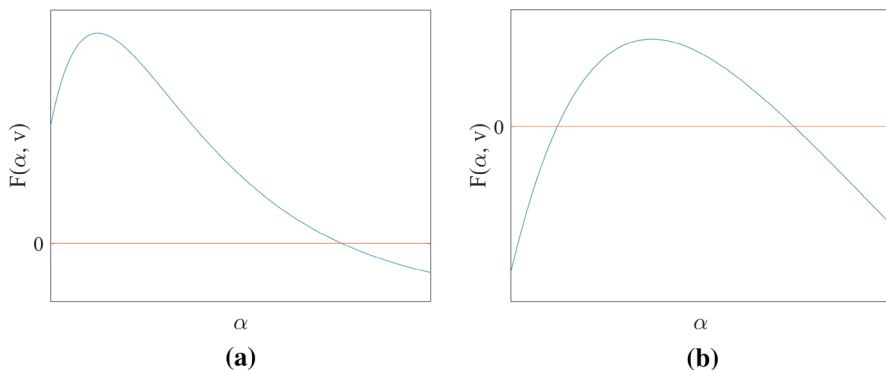
Fig. 1 Function $F(\alpha)$ has a global maximum if and only if $p/s > \max\{b_0/(c_0v), 1\}$: **a** $F(0) > 0$; **b** $F(0) < 0$ but $F(\alpha^*) > 0$ (color figure online)

(ii) Assume $p/s < 1$, then

(ii)-1 if $\frac{p}{s} < \frac{b_0}{c_0v}$, then $F(\alpha)$ has a unique critical point $\alpha^* > 0$ at which $F(\alpha)$ attains a minimum;

(ii)-2 if $\frac{p}{s} > \frac{b_0}{c_0v}$, then $F'(\alpha) > 0$ for all $\alpha > 0$ (hence, $F(0) < F(\alpha) < F(\infty)$ $= -d < 0$ for all $\alpha > 0$, which should be excluded).

From the above, we can see that only (i)-2 (i.e., $p/s > \max\{b_0/(c_0v), 1\}$) offers the scenario of local interior value α^* given by

$$\alpha^* = \frac{1}{p-s} \ln\left(\frac{pc_0v}{sb_0}\right) \tag{16}$$

at which the fitness function $F(\alpha)$ attains its global maximum. By the definition of ESS and CSS, it is easy to see that such strategy α^* is an ESS which is convergence stable. One can also check that both conditions (12) and (13) are satisfied. Lemma 3.1 implies that the persistence of prey's population requires $F(\alpha)$ to be positive. If $F(0)$ $= b_0 - d - c_0v > 0$, then the maximum $F(\alpha^*) > 0$; and even if $F(0) = b_0 - d - c_0v < 0$ meaning that the prey will go to extinction without any anti-predation response, it is possible to have $F(\alpha^*) > 0$ which shows that an anti-predation response can help the prey survive. See Fig. 1a, b for a demonstration.

We can interpret the above mathematical results from biological point of view. Note that the ratio p/s measures the relative effect of the anti-predation response on surviving the predation (benefit) as opposed to that on reducing the reproduction (cost). Thus, when p/s is small (large s and small p), the effect of reducing the predation is not as significant as the effect of reducing the reproduction, and hence, it seems to be preferable for the prey to take less response; this corresponds to the cases (i)-1 and (ii)-1 in which the maximum of $F(\alpha)$ is attained at $\alpha = 0$. When p/s is sufficiently large (i.e., $p/s > \max\{b_0/(c_0v), 1\}$), the effect of reducing the predation is more significant than the effect of reducing the reproduction, and hence, a positive and relatively larger response level should be favoured, and this corresponds to the cases (i)-2 and (ii)-2. Moreover, when the population grows to the steady state $F(\alpha^*)/a$ after the prey strain

with the ESS/CSS α^* having occupied the patch, it is also the maximal population size the species can reach.

Apparently, the value $b_0/(c_0v)$ plays an important role in determining the population dynamics of prey, which is the ratio of per capita birth rate to per capita death rate due to predation without anti-predation response. When the ratio is smaller than one, the existence of positive convergence stable ESS only requires $p/s > 1$. When the ratio is greater than one, the condition becomes $p/s > b_0/(c_0v) > 1$. If a species population is able to produce more offspring (meaning larger b_0), anti-predation behaviours are less likely to be developed. Moreover, the ratio $b_0/(c_0v)$ depends on the population of predator, while $p/s = (\tilde{p}v)/(\tilde{s}v) = \tilde{p}/\tilde{s}$ is only related to the prey species. When the number of predators is sufficiently small, indicating that the existence of predators does not threaten the survival of prey, such fear will not change the behaviours of prey. If there are too many predators meaning that predation risk is relatively high, the prey species will be driven/forced to develop some anti-predation strategies.

In this model, co-existence is impossible since $\theta(\alpha_w, \alpha_u)$ and $\theta(\alpha_u, \alpha_w)$ cannot be positive simultaneously. A successful invasion of mutant prey always leads to the extinction of resident prey and the mutant prey becomes new resident prey. This means that trait substitution occurs. In reality, evolution dynamics is typically much slower than the population dynamics. Thus, we further assume that the duration of the inter-strain (or inter-species) competitive interaction is much shorter than the mutation process, so that the population has approached a steady state before the appearance of new mutant. Repeating the trait substitution generates a sequence of trait values which converges to the ESS/CSS. Biologically speaking, an optimal anti-predation strategy is developed by mutation and natural selection.

The information concerning the adaptive dynamics of anti-predation strategy α can be illustrated graphically in the pairwise invasibility plot (PIP). See Fig. 2 for an example when a positive convergence stable ESS exists with the chosen parameter values satisfying $p/s > b_0/(c_0v) > 1$. The $\alpha_u - \alpha_w$ plane is divided by the curves where $\theta(\alpha_u, \alpha_w) = 0$. In the blue regions $\theta(\alpha_u, \alpha_w)$ is positive, corresponding to successful invasion by mutant, whereas in the white regions the invader fails since $\theta(\alpha_u, \alpha_w)$ is negative. The point where two curves intersect is consistent with the value given by (16). Such a strategy is both an ESS and a CSS.

Fig. 2 Pairwise invasibility plot for model (10) with trait α. Function $F(\alpha, v)$ is in the form of (15) and $b_0 = 5$, $d = 0.5$, $c_0v = 3.5$, $s = 1$, $p = 3$. The mutant can invade in the blue regions but the invader fails in the white regions. The intersection of two curves gives a convergence stable ESS $\alpha^* = 0.37$ (color figure online)
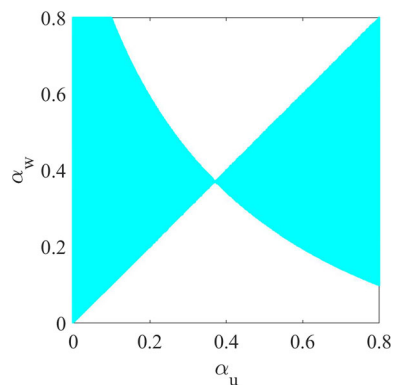
4 Model Analysis: With Dispersal

In this section, we consider the full model (8) with dispersals which are also affected by fear.

4.1 Equilibria and Stability

Firstly, we consider the trait α as a constant. System (8) admits only two equilibria: $E_0 = (0, 0)$ and $E_+ = (u_1^*, u_2^*)$, with u_1^* and u_2^* satisfying:

$$
\begin{aligned}
u_1^* &= \frac{au_2^*}{m(\alpha, v_1)} \left[u_2^* - \frac{F_2(\alpha, v_2) - m(\alpha, v_2)}{a} \right] =: \Pi_1(u_2^*), \\
u_2^* &= \frac{au_1^*}{m(\alpha, v_2)} \left[u_1^* - \frac{F_1(\alpha, v_1) - m(\alpha, v_1)}{a} \right] =: \Pi_2(u_1^*).
\end{aligned}
\tag{17}
$$

The first quadratic function Π_1 has two roots

$$
u_2 = 0 \quad \text{and} \quad u_2 = \frac{F_2(\alpha, v_2) - m(\alpha, v_2)}{a} =: \hat{u}_2,
$$

and the second function Π_2 also has two roots

$$
u_1 = 0 \quad \text{and} \quad u_1 = \frac{F_1(\alpha, v_1) - m(\alpha, v_1)}{a} =: \hat{u}_1.
$$

These two parabolas intersect at the origin. Moreover, when $\hat{u}_1 \geq 0$ or $\hat{u}_2 \geq 0$, the two curves always have a unique intersection in the interior of the first quadrant. When $\hat{u}_1 < 0$ and $\hat{u}_2 < 0$, there is an interior intersection in the first quadrant if and only if the slopes of two curves at the origin satisfy $\Pi_1'(0) \cdot \Pi_2'(0) < 1$, which is equivalent to $F_1(\alpha, v_1) F_2(\alpha, v_2) < F_1(\alpha, v_1) m(\alpha, v_2) + F_2(\alpha, v_2) m(\alpha, v_1)$. Hence, we have the following result on the existence of co-persistence equilibrium.

Theorem 4.1 *The system* (8) *has a unique positive equilibrium if and only if one of the following conditions holds:*

(i) $F_1(\alpha, v_1) \geq m(\alpha, v_1)$,
(ii) $F_2(\alpha, v_2) \geq m(\alpha, v_2)$,
(iii) $F_1(\alpha, v_1) < m(\alpha, v_1)$, $F_2(\alpha, v_2) < m(\alpha, v_2)$, *and* $F_1(\alpha, v_1) F_2(\alpha, v_2) < F_1(\alpha, v_1) m(\alpha, v_2) + F_2(\alpha, v_2) m(\alpha, v_1)$.

The Jacobian matrix for system (8) is given by

$$
\mathbf{J} = \begin{pmatrix} F_1(\alpha, v_1) - m(\alpha, v_1) - 2au_1 & m(\alpha, v_2) \\ m(\alpha, v_1) & F_2(\alpha, v_2) - m(\alpha, v_2) - 2au_2 \end{pmatrix}. \tag{18}
$$

At the trivial equilibrium E_0, it becomes

$$
\mathbf{J}(E_0) = \begin{pmatrix} F_1(\alpha, v_1) - m(\alpha, v_1) & m(\alpha, v_2) \\ m(\alpha, v_1) & F_2(\alpha, v_2) - m(\alpha, v_2) \end{pmatrix}. \tag{19}
$$

Fig. 3 The solid curve is implicitly defined by $F_1(\alpha, v_1)F_2(\alpha, v_2) = F_1(\alpha, v_1)m(\alpha, v_2) + F_2(\alpha, v_2)m(\alpha, v_1)$ for $F_1(\alpha, v_1) < m(\alpha, v_1)$, below which E_0 is asymptotically stable. The region above this curve is where the trivial equilibrium E_0 is unstable which is the same region for (F_1, F_2) where the positive equilibrium E_+ exists (color figure online)
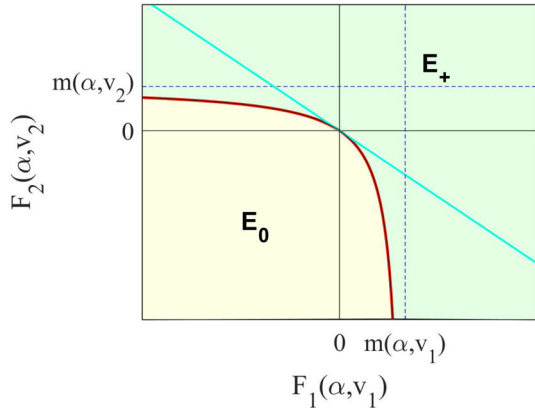
Thus, the trivial equilibrium E_0 is locally asymptotically stable if

$$tr(\mathbf{J}(E_0)) = F_1(\alpha, v_1) - m(\alpha, v_1) + F_2(\alpha, v_2) - m(\alpha, v_2) < 0,$$
$$det(\mathbf{J}(E_0)) = F_1(\alpha, v_1)F_2(\alpha, v_2) - F_1(\alpha, v_1)m(\alpha, v_2) - F_2(\alpha, v_2)m(\alpha, v_1) > 0.$$
$$(20)$$

As shown graphically in Fig. 3, this condition represents the region under the solid curve defined by the equation

$$F_1(\alpha, v_1)F_2(\alpha, v_2) = F_1(\alpha, v_1)m(\alpha, v_2) + F_2(\alpha, v_2)m(\alpha, v_1), \qquad (21)$$

or written in the explicit form,

$$F_2(\alpha, v_2) = \frac{m(\alpha, v_1)m(\alpha, v_2)}{F_1(\alpha, v_1) - m(\alpha, v_1)} + m(\alpha, v_2), \qquad (22)$$

for $F_1(\alpha, v_1) < m(\alpha, v_1)$ on the F_1–F_2 plane. It is not difficult to observe that conditions in (20) is precisely the conditions that exclude the existence of a positive equilibrium.

Remark 4.1 Notice that the tangent line of the curve at $(F_1(\alpha, v_1), F_2(\alpha, v_2)) = (0, 0)$ is $F_1(\alpha, v_1)m(\alpha, v_2) + F_2(\alpha, v_2)m(\alpha, v_1) = 0$, shown as the thick solid straight line in Fig. 3. Hence, the condition in Theorem 4.1 for the existence of positive equilibrium can be equivalently stated as

either (A) $F_1(\alpha, v_1)m(\alpha, v_2) + F_2(\alpha, v_2)m(\alpha, v_1) \geq 0,$
  or (B) $0 > F_1(\alpha, v_1)m(\alpha, v_2) + F_2(\alpha, v_2)m(\alpha, v_1) > F_1(\alpha, v_1)F_2(\alpha, v_2).$
$$(23)$$

The advantage of these equivalent statements is that they are expressed in terms of the weighted total fitness $F_1(\alpha, v_1)m(\alpha, v_2) + F_2(\alpha, v_2)m(\alpha, v_1)$, which is the

total of the two local fitness functions mediated by the dispersal strengths. Such a weighted total obviously combines the local fitness and the dispersal effect, and is thus a biologically meaningful measure for the total fitness of the prey on the two patches.

As for the positive equilibrium $E_+ = (u_1^*, u_2^*)$, recall that u_1^* and u_2^* satisfy (17) which can be written as

$$\frac{m(\alpha, v_1)u_1^*}{u_2^*} = au_2^* - (F_2(\alpha, v_2) - m(\alpha, v_2)),$$

$$\frac{m(\alpha, v_2)u_2^*}{u_1^*} = au_1^* - (F_1(\alpha, v_1) - m(\alpha, v_1)).$$

Using these to rewrite the diagonal entries of $\mathbf{J}(E_+)$, we have

$$\mathbf{J}(E_+) = \begin{pmatrix} -\dfrac{m(\alpha, v_2)u_2^*}{u_1^*} - au_1^* & m(\alpha, v_2) \\ m(\alpha, v_1) & -\dfrac{m(\alpha, v_1)u_1^*}{u_2^*} - au_2^* \end{pmatrix} \tag{24}$$

with

$$tr(\mathbf{J}(E_+)) = -\frac{m(\alpha, v_2)u_2^*}{u_1^*} - au_1^* - \frac{m(\alpha, v_1)u_1^*}{u_2^*} - au_2^* < 0,$$

$$det(\mathbf{J}(E_+)) = \frac{am(\alpha, v_2)(u_2^*)^2}{u_1^*} + \frac{am(\alpha, v_1)(u_1^*)^2}{u_2^*} + a^2 u_1^* u_2^* > 0.$$

Hence, the positive equilibrium is always locally asymptotically stable as long as it exists.

Indeed, we can prove that for this model system (8), the local asymptotic stability of an equilibrium also implies the global asymptotic stability. To this end, we just need to show that there is no periodic solution of system (8) by using the Dulac criterion. Set $B(u_1, u_2) = 1/(u_1 u_2)$, then we have

$$G_1(u_1, u_2) := B(u_1, u_2)\frac{du_1}{dt} = \frac{F_1(\alpha, v_1) - m(\alpha, v_1) - au_1}{u_2} + \frac{m(\alpha, v_2)}{u_1},$$

$$G_2(u_1, u_2) := B(u_1, u_2)\frac{du_2}{dt} = \frac{F_2(\alpha, v_2) - m(\alpha, v_2) - au_2}{u_1} + \frac{m(\alpha, v_1)}{u_2}.$$

Since

$$\frac{\partial G_1}{\partial u_1} + \frac{\partial G_2}{\partial u_2} = -\frac{a}{u_2} - \frac{m(\alpha, v_2)}{u_1^2} - \frac{a}{u_1} - \frac{m(\alpha, v_1)}{u_2^2}$$

is not identically zero and does not change sign in $\mathbb{R}_+^2$, there is no periodic orbit. Hence, by the Poincaré–Bendixson theory of planar dynamical systems, a locally asymptotically stable equilibrium is also globally asymptotically stable.

Summarizing the above analysis, we have obtained the following global threshold result.

Theorem 4.2 *The following statements hold:*

(i) *If condition* (20) *holds, then for any initial point* $[u_1(0), u_2(0)] \in \mathbb{R}_+^2$, *the corresponding solution of* (8) *satisfies* $\lim_{t \to \infty} u_1(t) = \lim_{t \to \infty} u_2(t) = 0$.

(ii) *If condition* (20) *is violated [i.e.,* (23) *holds], then the trivial equilibrium becomes unstable, and there is a unique positive equilibrium E_+ (representing the prey's co-persistence on both patches) which is globally asymptotically stable.*

Recall that in the absence of dispersal, the species survives in *both patches* if and only if $F_1(\alpha, v_1) > 0$ and $F_2(\alpha, v_2) > 0$. However, with the dispersal, the range of $F_1(\alpha, v_1)$ and $F_2(\alpha, v_2)$ for co-persistence of the species in both patches has obviously been *enlarged*, as shown in Fig. 3. Particularly, co-existence in both patches is also possible even if *one of the fitness functions is negative*, and this clearly and explicitly shows the positive role of dispersal on maintaining the population persistence.

Although dispersal can enhance the chance to survive, it does not necessarily mean that higher dispersal rate is always better. When the dispersal rates are greater than the corresponding linear net growth rates (i.e., when $m(\alpha, v_i) > F_i(\alpha, v_i)$ for $i = 1, 2$), there are ranges for parameters within which the species will be driven to extinction. See the region under the solid curve and located in the two stripes $F_1(\alpha, v_1) \in (0, m(\alpha, v_1))$ and $F_2(\alpha, v_2) \in (0, m(\alpha, v_2))$ in the F_1–F_2 plane as shown in Fig. 3. Or to be more explicit, we consider a special case where dispersal rate is independent of the populations of predator, denoted as $m(\alpha)$. Then, the conditions in (23) for the persistence of prey on both patches are simplified to

$$\text{either (A*)} \quad F_1(\alpha, v_1) + F_2(\alpha, v_2) \geq 0,$$

$$\text{or (B*)} \quad F_1(\alpha, v_1) + F_2(\alpha, v_2) < 0 \quad \text{and} \quad 0 < m(\alpha) < \frac{F_1(\alpha, v_1) F_2(\alpha, v_2)}{F_1(\alpha, v_1) + F_2(\alpha, v_2)}.$$

$$(25)$$

In Case (B*), there is an explicit upper bound for the dispersal strength $m(\alpha)$. Therefore, in such a special case, when the total fitness is positive, the species always persists on both patches even if one local fitness is negative (patch quality is very poor), as long as there is dispersal ($m(\alpha) > 0$) regardless of how small and how large it is. However, if the total fitness is negative, the species will eventually die out on both patches if the dispersal rate exceeds the threshold given in (25), but will persist if the prey maintains a mild dispersal rate.

Combining the above results with the dependence of $F_i(\alpha, v_i)$ and $m(\alpha, v_i)$ on α for $i = 1, 2$, one then can explore the effect of the anti-predation response level α on the prey's population dynamics. To illustrate possible outcomes, we choose the following particular functions,

$$F_i(\alpha, v_i) = b_{0i} e^{-\tilde{s}\alpha v_i} - d_i - c_0 v_i e^{-\tilde{p}\alpha v_i}, \quad i = 1, 2, \tag{26}$$

$$m(\alpha, v_i) = m_0 e^{-\tilde{q}\alpha v_i}, \quad i = 1, 2, \tag{27}$$
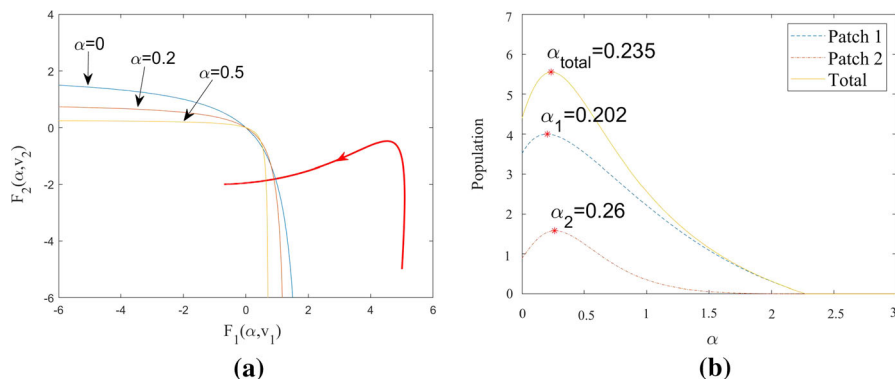
Fig. 4 The effect of anti-predation response level α on the prey's population dynamics. **a** The curves defined by (22) with different values of α, which separate the stability region of the positive equilibrium E_+ from that of the trivial equilibrium E_0. The red curve with arrow represents the trajectory of $[F_1(\alpha, v_1), F_2(\alpha, v_2)]$ when α increases from 0 to 3.5. **b** The dependence of stable population sizes on α, marked with the strategy values at which the populations are maximized. Other parameter values are: $b_{01} = 10$, $b_{02} = 5$, $d_1 = 1$, $d_2 = 2$, $c_0 = 0.04$, $v_1 = 100$, $v_2 = 200$, $\tilde{s} = 0.01$, $\tilde{p} = 0.03$, $m_0 = 2$, $\tilde{q} = 0.02$, and $a = 1$ (color figure online)

which satisfy all those assumptions proposed in Sect. 2. Figure 4a shows the variation of curve defined by (22) with respect to anti-predation strategy α. Recall that this curve separates the stability region of the trivial equilibrium E_0 from the region where the positive equilibrium E_+ is globally asymptotically stable. When α increases, the stability region of the positive equilibrium is enlarged, and the pair of values $[F_1(\alpha, v_1), F_2(\alpha, v_2)]$ moves along the red curve from the stability region of E_+ into the stability region of E_0. Consequently, the population on two patches converges to a positive steady state for small α, but prey on both patches go to extinction when α exceeds some critical point. The stable population sizes are plotted in Fig. 4b, marked with the strategy values when populations reach their maxima. Enhancing anti-predation response level is beneficial to population size when α is small, then it becomes detrimental. Such effect is not synchronous on the two patches.

4.2 Evolution of Anti-predation Strategy

In this subsection, we move on to study the evolution of anti-predation strategy α.

4.2.1 Invasion Analysis

Due to the presence of dispersal between the patches, adopting the same invasibility analysis as in Sect. 3 leads to a four-dimensional ODE system,

$$
\begin{cases}
\dfrac{du_1}{dt} = u_1\left[F_1(\alpha_u, v_1) - a(u_1 + w_1)\right] + m(\alpha_u, v_2)u_2 - m(\alpha_u, v_1)u_1 \\[2mm]
\dfrac{du_2}{dt} = u_2\left[F_2(\alpha_u, v_2) - a(u_2 + w_2)\right] + m(\alpha_u, v_1)u_1 - m(\alpha_u, v_2)u_2 \\[2mm]
\dfrac{dw_1}{dt} = w_1\left[F_1(\alpha_w, v_1) - a(u_1 + w_1)\right] + m(\alpha_w, v_2)w_2 - m(\alpha_w, v_1)w_1, \\[2mm]
\dfrac{dw_2}{dt} = w_2\left[F_2(\alpha_w, v_2) - a(u_2 + w_2)\right] + m(\alpha_w, v_1)w_1 - m(\alpha_w, v_2)w_2.
\end{cases}
\tag{28}
$$

The ability of the mutant to invade can be determined from the eigenvalues of the Jacobian matrix of the augmented system at boundary equilibrium $(u_1^*, u_2^*, 0, 0)$ with u_1^* and u_2^* being solved from (17):

$$
\mathbf{J} = \begin{pmatrix} \mathbf{J_{11}} & \mathbf{J_{12}} \\ \mathbf{0} & \mathbf{J_{22}} \end{pmatrix}.
\tag{29}
$$

This is an upper triangular matrix, so the eigenvalues are simply those of the two 2×2 block-diagonal elements $\mathbf{J_{11}}$ and $\mathbf{J_{22}}$. The matrix $\mathbf{J_{11}}$ is identical to the Jacobian matrix $\mathbf{J}(E_+)$ given by (24). Since we are only interested in resident prey populations that are at a stable positive equilibrium, the two eigenvalues of $\mathbf{J_{11}}$ must have negative real parts. Thus, the local stability fully depends on the dominant eigenvalue of matrix $\mathbf{J_{22}} = \begin{pmatrix} A & B \\ C & D \end{pmatrix}$,

$$
\lambda = \frac{1}{2}\left(A + D + \sqrt{(A - D)^2 + 4BC}\right),
\tag{30}
$$

where

$$
\begin{aligned}
A &= F_1(\alpha_w, v_1) - m(\alpha_w, v_1) - au_1^*, \quad B = m(\alpha_w, v_2), \\
C &= m(\alpha_w, v_1), \quad D = F_2(\alpha_w, v_2) - m(\alpha_w, v_2) - au_2^*.
\end{aligned}
$$

A mutant prey with strategy α_w can invade the resident population with strategy α_u provided that $\lambda > 0$. Hence, we choose λ as the invasion exponent because it directly determines whether the mutant strain, when being rare, will grow or decay (invade or not). An evolutionary singular strategy $\alpha_u = \alpha^*$ is a solution to the equation

$$
\left.\frac{\partial \lambda(\alpha_u, \alpha_w)}{\partial \alpha_w}\right|_{\alpha_w = \alpha_u} = 0.
\tag{31}
$$

This strategy is an ESS if

$$
\left.\frac{\partial^2 \lambda(\alpha_u, \alpha_w)}{\partial \alpha_w^2}\right|_{\alpha_w = \alpha_u = \alpha^*} < 0;
\tag{32}
$$

Fig. 5 Pairwise invasibility plot for model (28) with trait α. The blue areas correspond to $\lambda > 0$ when the mutant can invade, and in the white areas $\lambda < 0$ implying that the mutant dies out (color figure online)
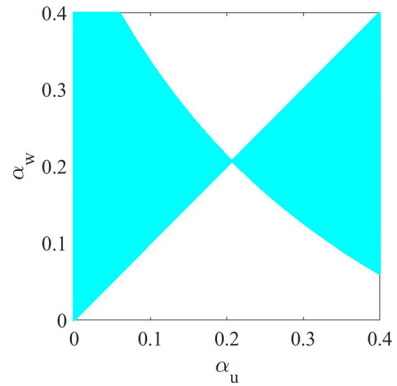
and α^* is convergence stable if

$$
\frac{\partial^2 \lambda(\alpha_u, \alpha_w)}{\partial \alpha_u^2}\bigg|_{\alpha_w = \alpha_u = \alpha^*} > \frac{\partial^2 \lambda(\alpha_u, \alpha_w)}{\partial \alpha_w^2}\bigg|_{\alpha_w = \alpha_u = \alpha^*}. \tag{33}
$$

See Diekmann (2004) for details. It is not easy to explore further explicitly by applying these criteria. This is because of the complexity of $\lambda(\alpha_u, \alpha_w)$—it depends on $u_1^*(\alpha_u)$ and $u_2^*(\alpha_u)$ which are determined by but cannot be explicitly solved from (17).

However, we can still gain some information about the adaptive dynamics of anti-predation strategy α by sketching the pairwise invasibility plot numerically. An example is illustrated in Fig. 5 using the particular functions $F_i(\alpha, v_i)$ and $m(\alpha, v_i)$ given by (26) and (27) and the same parameter values as in Fig. 4. The $\alpha_u - \alpha_w$ plane is partitioned according to the signs of invasion exponent λ defined by (30). We can easily tell that the singular point at which the two curves of neutrality intersect is an ESS. Even though the condition for mutual invasibility (Diekmann 2004),

$$
\frac{\partial^2 \lambda(\alpha_u, \alpha_w)}{\partial \alpha_u^2}\bigg|_{\alpha_w = \alpha_u = \alpha^*} > -\frac{\partial^2 \lambda(\alpha_u, \alpha_w)}{\partial \alpha_w^2}\bigg|_{\alpha_w = \alpha_u = \alpha^*}, \tag{34}
$$

is hard to check, it seems to be impossible since the plot in Fig. 5 is symmetric about the line $\alpha_w = \alpha_u$. One may expect the dynamics to be monomorphic.

We have seen there are some shortcomings of invasibility analysis. This motivates us to employ an alternative method, that is, considering an augmented system with the anti-predation response level α being another variable. We explore this method in the next subsection.

4.2.2 Adaptive Dynamics Without Time Scale Separation

Assume that the prey has complete knowledge about the surrounding environment and always adapts its behaviour to increase fitness. Thus, the evolution of $\alpha = \alpha(t)$ with respect to time should be towards the direction of increasing the fitness of the

prey species. This can be reflected by assuming that the relative change rate of α is proportional to the gradient of the fitness with respect to α, that is,

$$\frac{d\alpha}{dt} = \sigma\alpha\frac{\partial\Phi}{\partial\alpha}, \tag{35}$$

where Φ accounts for some measure of fitness for the prey and $\sigma > 0$ represents the speed of evolution. It is easy to see that the solution to (35) remains positive, given any positive initial value. We point out that here our trait variable α is within $[0, \infty)$ in comparison to some previous used replicator equations of the form $\alpha'(t) = \sigma\alpha(1 - \alpha)\frac{\partial\Phi}{\partial\alpha}$ where α is confined to [0, 1]. See, e.g., Takeuchi et al. 2009; Wang et al. 2016 and some references therein.

To gain some motivation for the fitness function Φ, let us revisit the case without dispersal discussed in Sect. 3, using this alternative idea of evolving strategy α (rather than comparing two different constant values for α as done in Sect. 3). Then, instead of the model (10) that describes the competition between resident prey and mutants with different anti-predation response levels, we may consider following new system consisting of Eq. (9) for the population and Eq. (35) for strategy:

$$\begin{cases} \dfrac{du}{dt} = u\left[F(\alpha, v) - au\right], \\ \dfrac{d\alpha}{dt} = \sigma\alpha\dfrac{\partial\Phi}{\partial\alpha}, \end{cases} \tag{36}$$

where σ should be relatively small since speed of evolution is much slower than the demographic process. As discussed in Sect. 3, $F(\alpha, v)$ is a measure of fitness for the species and hence, is a natural candidate for Φ. With this choice of $\Phi = F(\alpha, v)$, the second equation in (36) is decoupled from the first equation, and hence can be dealt with independently. Besides $\alpha = 0$, all singular points of Φ such that $\frac{\partial\Phi}{\partial\alpha} = 0$ are fixed points of the strategy equation. When $\alpha(t)$ starting from any initial value eventually converges to one fixed point α^*, the population approaches to its steady state accordingly based on the sign of $F(\alpha^*, v)$. If $F(\alpha, v)$ is in the form of (15) for $p/s > \max\{b_0/(c_0v), 1\}$ which is a one-hump function, then α^* is the point at which $F(\alpha, v)$ attains its maximum. This result is consistent with what we obtained in Sect. 3.

Now we combine the strategy equation (35) with the two-patch population model (8) with dispersals. The first and most important thing is to determine what function is appropriate to be the fitness Φ. From the discussion in Remark 4.1, we have seen that total fitness mediated by the dispersals, that is $F_1(\alpha, v_1)m(\alpha, v_2) + F_2(\alpha, v_2)m(\alpha, v_1)$, is of both mathematical and biological significance. Thus, similar to the choice of $\Phi = F(\alpha, v)$ for model (36), we may use the above quantity as a measure of fitness for the prey in two-patch environment. Then, we are led to consider the system given below:

(a) Fitness function

(b) Anti-predation response level α
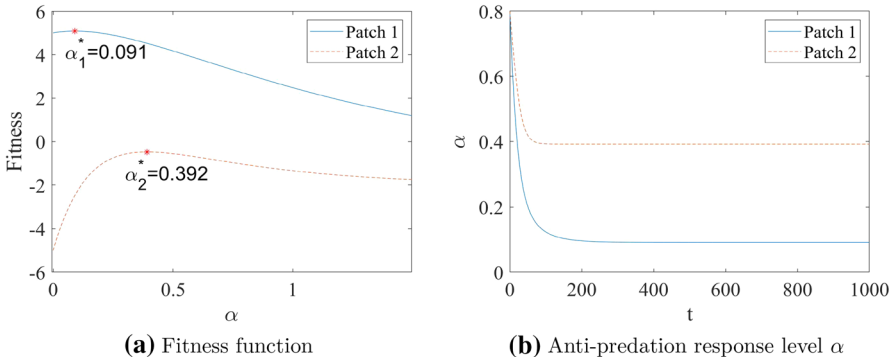
Fig. 6 The fitness function $F_1(\alpha, v_1)$ and $F_2(\alpha, v_2)$ and convergent dynamics of anti-predation response level $\alpha(t)$ on the two patches which are *not connected* by dispersals (color figure online)

$$
\begin{cases}
\dfrac{du_1}{dt} = u_1\,[F_1(\alpha, v_1) - au_1] + m(\alpha, v_2)u_2 - m(\alpha, v_1)u_1, \\[2mm]
\dfrac{du_2}{dt} = u_2\,[F_2(\alpha, v_2) - au_2] + m(\alpha, v_1)u_1 - m(\alpha, v_2)u_2, \\[2mm]
\dfrac{d\alpha}{dt} = \sigma\alpha\,\dfrac{\partial}{\partial\alpha}\,[F_1(\alpha, v_1)m(\alpha, v_2) + F_2(\alpha, v_2)m(\alpha, v_1)].
\end{cases}
\tag{37}
$$

The strategy equation is also decoupled from the population equations, and its dynamics depends on the choices of $F_i(\alpha, v_i)$ and $m(\alpha, v_i)$, $i = 1, 2$. Without specifying these functions, one can hardly obtain any conclusive results. Thus, in order to illustrate how the anti-predation response level α evolves along time, we use the functions (26) and (27) again and conduct some numeric investigations with the same parameter values as those used in Sect. 4.1 and $\sigma = 0.01$.

If the two patches are *not* connected by dispersals, the prey evolves separately on each patch according to system (36) with different parameter values. The fitness functions $F_1(\alpha, v_1)$ and $F_2(\alpha, v_2)$ are of the same form as (15), and hence, their behaviours are also as demonstrated in Fig. 1 with the given parameter values satisfying $\tilde{p}/\tilde{s} > \max\{b_{0i}/(c_0 v_i), 1\}$ for $i = 1, 2$. Their maximal values are reached at different critical points α_1^* and α_2^*. As shown in Fig. 6, the anti-predation response level α in each patch evolves towards the corresponding critical points α_1^* and α_2^*.

In the *presence of dispersals*, the weighted total fitness with the same parameter values also has a global maximum attained at point α^{1*}, as plotted in Fig. 7a, which is in between of α_1^* and α_2^*. The convergence of $\alpha(t)$ to α^{1*} for some initial values near α^{1*} is numerically demonstrated in Fig. 7b, indicating that α^{1*} at least is a local attractor.

Besides the total fitness mediated by dispersals, there are other choices for the fitness function Φ. In principle, anything that captures that biological meaning and in the mean time, is mathematically tractable can be used to measure the fitness. For example, as was used in Wang and Zou (2017), the instant growth rate of the total population of the prey species,

(a) Fitness function

(b) Anti-predation response level α
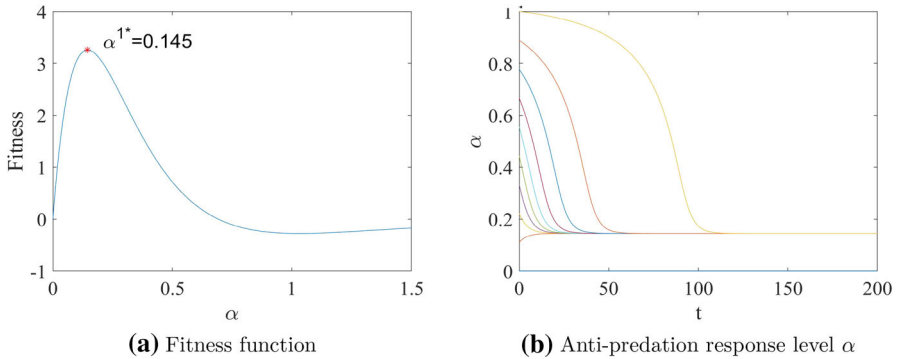
Fig. 7 The fitness function is taken as the total fitness mediated by dispersals. The anti-predation response level $\alpha(t)$ converges to the point that maximizes this fitness function (color figure online)

$$\Phi = \frac{\mathrm{d}u_1}{\mathrm{d}t} + \frac{\mathrm{d}u_2}{\mathrm{d}t}$$
$$= u_1 \left[F_1(\alpha, v_1) - au_1 \right] + u_2 \left[F_2(\alpha, v_2) - au_2 \right]. \tag{38}$$

Accordingly, the equation governing the strategy's evolution becomes

$$\frac{\mathrm{d}\alpha}{\mathrm{d}t} = \sigma\alpha \left[u_1 \frac{\partial F_1(\alpha, v_1)}{\partial \alpha} + u_2 \frac{\partial F_2(\alpha, v_2)}{\partial \alpha} \right]. \tag{39}$$

Unlike in the above two examples, now we have a *coupled* system for the strategy and the populations. It becomes impossible to plot the fitness function since it also varies with time. But we can still explore the dynamics of $\alpha(t)$ numerically. With the same function forms in (26) and (27) and the same values of the parameters involved, the adaptive dynamics of $\alpha(t)$ are illustrated in Fig. 8b. We can see that the variable $\alpha(t)$ beginning within the same range for initial values used in Fig. 7 converges to a value α^{2*} which is different from α^{1*}. Additionally, α^{2*} maximizes the limit fitness function when the populations reach steady state, as shown in Fig. 8a. We also observe that the convergence of $\alpha(t)$ is faster than that in previous example.

From the above numerical explorations, we have seen that for both choices of Φ, the trait variable $\alpha(t)$ demonstrates convergent dynamics. However, the convergence speed and the destination values α^{1*} and α^{2*} can be different for different Φ. This is because those fitness functions have different emphases and hence, may not be maximized uniformly. Moreover, none of the critical points matches the ESS obtained from the pairwise invasibility plot shown in Fig. 5. We point out that the numerical results on the convergence of $\alpha(t)$ to a critical value α^{i*} demonstrated in Figs. 7b and 8b, respectively, do not depend on the initial populations.

We are also interested to the final populations of prey on both patches when optimal strategy α^{i*} is reached. With the same parameter values used for Figs. 6, 7 and 8, numerical results for the populations are displayed in Fig. 9 which corresponds to the scenarios illustrated above: (a) no dispersals (Fig. 6), (b) dispersal considered with total fitness mediated by dispersals (Fig. 7) and (c) dispersal considered with fitness being

(a) Fitness function

(b) Anti-predation response level α
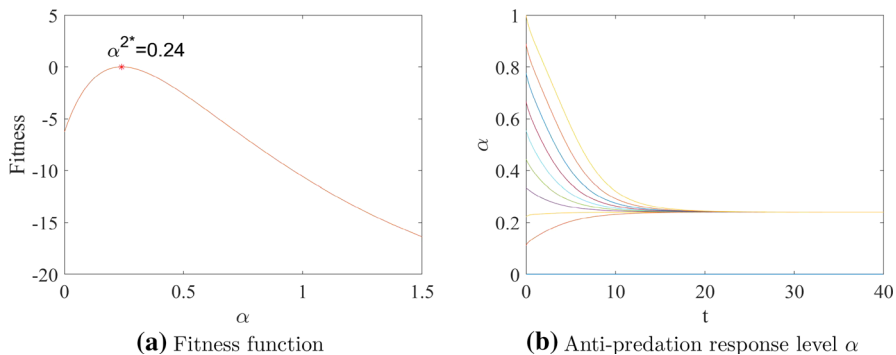
Fig. 8 The fitness function is taken as the instant total growth rate of the prey on two patches given by (38) which also varies with time. The anti-predation response level $\alpha(t)$ converges to a different value from that in Fig. 7b, which maximizes the limit fitness function when populations reach steady state as shown in the left graph (color figure online)

the instant total growth rate (Fig. 8). From the numerical results given in Fig. 9, we see that when dispersals between the two patches are not allowed, the prey's population can only persist in patch 1 since $F_1(\alpha_1^*, v_1) > 0$ and $F_2(\alpha_2^*, v_2) < 0$; but if the individuals of prey are free to move between the two patches, the prey coexists on both patches with the population size in patch 1 being higher than that in patch 2. Moreover, in the presence of dispersal, the total population in the steady state is larger than that in the case without dispersals, no matter which fitness function is adopted. Comparing with the results obtained in Fig. 4, we observe that none of the optimal strategies maximizes the population of prey. Such a phenomenon that an optimal strategy does not necessarily maximize the total population was also observed in previous studies. For example, in Hastings (1983), it was shown that the ESS dispersal strategy does not maximize the total population of the species on two patches; and in Lundberg (2013), it was also observed that the maximal population deviates from the solution with an ESS migration probability.

5 Conclusion and Discussion

Motivated by some recent works about indirect effect on predator–prey systems, we have proposed a mathematical model to examine the impact of fear on the population dynamics of prey. Unlike in Wang et al. (2016) where only the cost of the anti-predation response (reducing reproduction) was considered, here we have also considered the benefit of such a response for surviving the predation. Both the cost and benefit functions depend on the anti-predation response level and the population of predator. However, in other works concerning about the evolution of predator–prey interactions, the responses are only density independent (see Abrams 1986, 1990; Křivan 2007; Zu and Takeuchi 2012 for examples). In addition, we also have considered the fear effect on the dispersal strategy of prey under predation risk. In other words, we have incorporated the fear effects in three factors: reproduction, predation and dispersion. To this end, we have considered a two-patch environment by assuming that the habitat of a prey consists of two discrete regions with individuals being able

(a) No dispersal

(b) Φ is the total fitness mediated by dispersals

(c) Φ is the instant total growth rate
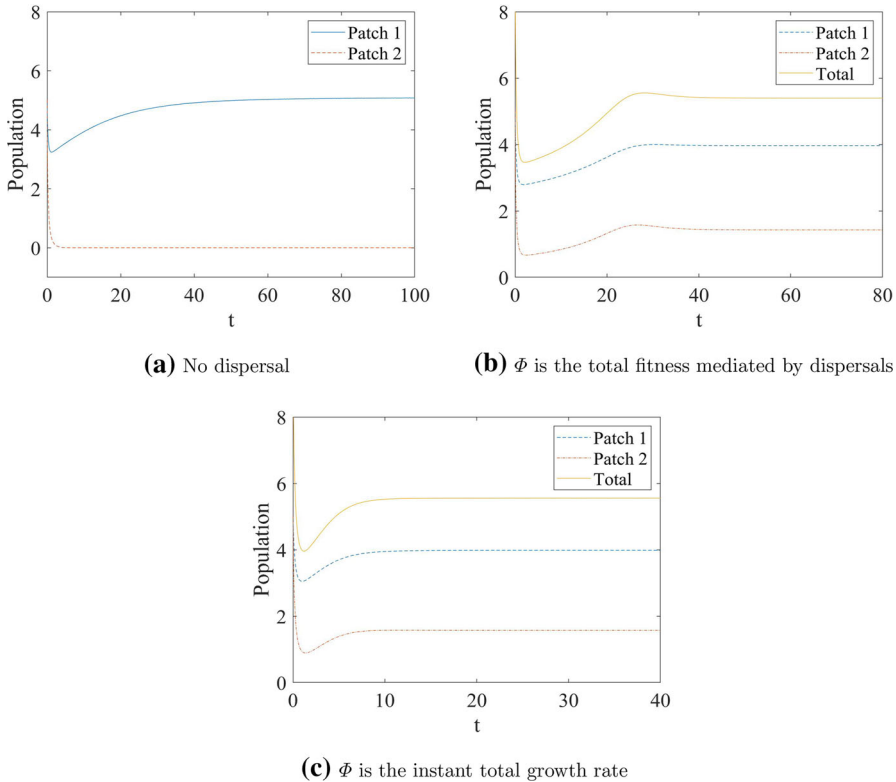
Fig. 9 The dynamics of prey's population for systems (36), (37) and (8)–(39). The initial values are $[u_1(0), u_2(0), \alpha(0)] = [5, 5, 0.8]$ (color figure online)

to disperse between the two regions. The unaffected dispersal rates are assumed to be symmetric since we are focused on the effect of fear and the anti-predation trait.

We start from a special case when there is no dispersal between the patches. Our results show that the optimal anti-predation response level α depends on whether its effect on *reducing the predation* is more or less significant than its effect on *reducing the reproduction*. For the former, there is a continuously stable strategy (which is both an ESS and a CSS) $\alpha^* > 0$ (see Figs. 1, 2), while for the latter, no response $\alpha = 0$ should be favoured. See Sect. 3 for detailed discussion. For the case when the patches are connected through dispersal of the prey, our results indicate that the dispersal can enhance the co-persistence of the prey in the two patches. This is clearly and visually demonstrated in Fig. 3 and is also discussed in detail after Theorem 4.2 in Sect. 4. If a particular form of the dispersal function $m(\alpha, v)$ is given (e.g., by (27) or some other functions satisfying (7)), one may further explore to obtain more detailed results on how α affects the co-persistence region in the F_1–F_2 plane. The numerical simulation displayed in Fig. 4 is provided as an example.

We continued to study the evolution of anti-predation response level α by invasibility analysis in Sect. 4.2.1. The criteria, however, are not practically useful. Alternatively, we let the trait α be another variable evolving with respect to time,

which leads to a model given by a system of three ordinary differential equations. The replicator equation governing the direction of evolution depends on a fitness function Φ. We have considered two particular forms of this Φ: (i) the total fitness mediated by dispersals which comes up in our analysis for the population system (see Sect. 4.1); (ii) the instant growth rate of the total population on both patches (motivated by Wang and Zou 2017). However, we have only numerically explored the model to see how the response level (as a trait variable) evolves with time, and the results at least indicate local convergence to a positive equilibrium of the full model with the response level $\alpha(t)$ evolving towards a positive value. This implies the existence of an optimal anti-predation response level. More rigorous and thorough analysis is still needed in order to obtain more detailed (explicit) qualitative and quantitative results.

As we pointed out in the numerical examples, there are many choices for the fitness functions in the extensive literatures of adaptive dynamics and evolutionary dynamics, and we just tried two. Other quantities, like the basic reproduction ratio, life span and basic depression ratio, are also often considered by researchers. When choosing functions to measure fitness, besides the main biological feature(s), mathematical convenience is often a main consideration. We believe that the biological species as well as the biological problem under consideration should also make some difference(s). It would not be surprising to see that the strategy variable $\alpha(t)$ would evolve to different positive values when different fitness functions are chosen.

In this paper, we have studied the evolutionary dynamics in two ways: adaptive dynamics with time scale separation (in Sects. 3, 4.2.1) and adaptive dynamics without time scale separation (in Sect. 4.2.2). By the former approach, the changes of trait are from mutation and natural selection and the process is graphically demonstrated by the pairwise invasibility plot. The critical strategies ESS and CSS are defined based on invasibility, associating with the stability/instability of corresponding competition system. The conditions for ESS and CSS have been proposed in previous works, but direct application may hardly provide any information due to the complexity of our model. The latter approach, however, clearly shows the direction of evolution, and the resulted system is more tractable in mathematics. Even though our results derived from the two methods are not quantitatively equivalent, we believe that there exists such a fitness function leading to the same evolutionary destination as the invasion method.

We have assumed in this paper that the fear effect decreases the mobility of the prey, reflected by the assumption (7) for the dispersal function $m(\alpha, v_i)$, and this assumption has those species that have refuges as prototypes of the prey species. On the other hand, there are prey species that have moving advantages (such as birds), for which, perceived predation risk would increase their dispersal rates (actively escaping from predators, or predator-taxis). For such species, in contrast to (7), the dispersal function $m(\alpha, v_i)$ would be an increasing function of both α and v_i. We will explore this case in another work. For the spatially continuum case, a predator-taxis diffusion mechanism has been discussed in Wang and Zou (2018).

Finally, we remark that in our model in this paper, the population of predators is assumed to remain constant. Although there are numerous situations that fit in such a scenario (e.g., when the predator is a generalist), a case where the predator population is not a constant may intrigue further extensions. This will increase the dimension of the model system and consequently, increase the difficulty level of analysis. In the

meanwhile, the model may present richer dynamics. Considering a specialist predator living in both patches, its populations decay exponentially in the absence of prey, governed by the following equations,

$$
\begin{cases}
\dfrac{dv_1}{dt} = \xi c(\alpha_u, v_1)u_1 v_1 + \xi c(\alpha_w, v_1)w_1 v_1 - d_v v_1, \\[2mm]
\dfrac{dv_2}{dt} = \xi c(\alpha_u, v_2)u_2 v_2 + \xi c(\alpha_w, v_2)w_2 v_2 - d_v v_2,
\end{cases}
\tag{40}
$$

where $\xi > 0$ denotes ingestion efficiency and $d_v > 0$ is the natural death rate. Assume that predators are not able to move between the patches. Combining these two predator equations with model system (28) and using the particular functions (26) and (27), numerical examples of population dynamics are shown in Figs. 10 and 11, corresponding to one-patch and two-patch environment, respectively. Unlike models (10) and (28) with constant predator populations showing monomorphic dynamics, co-existence of prey using different strategies is observed in the augmented model. Hence, evolutionary branching is possible. We leave this for future research projects.

Fig. 10 Population dynamics in an isolated patch for the case of a specialist predator. The parameter values are $a = 1$, $b_0 = 5$, $d = 0.5$, $c_0 = 0.35$, $\tilde{s} = 0.1$, $\tilde{p} = 0.3$, $\alpha_u = 0.1$, $\alpha_w = 0.7$, $d_v = 0.3$, $\xi = 0.2$; and the initial point is $[u(0), w(0), v(0)] = [5, 5, 5]$ (color figure online)
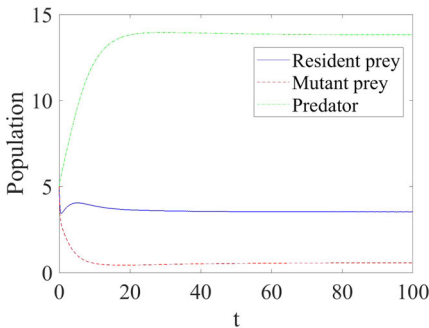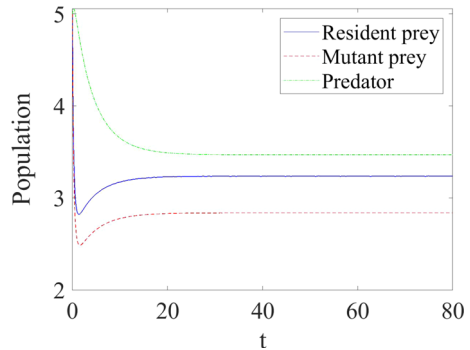
(a) Patch 1
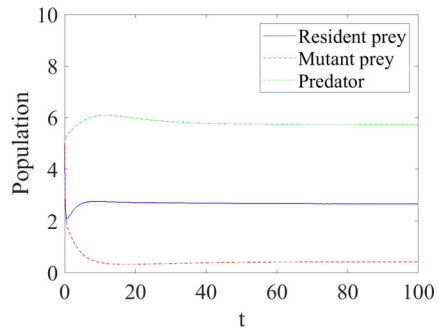
(b) Patch 2

Fig. 11 Population dynamics in a two-patch environment for the case of a specialist predator. The parameter values are $a = 1$, $b_{01} = 10$, $b_{02} = 5$, $d_1 = 0.5$, $d_2 = 0.3$, $c_0 = 0.4$, $\tilde{s} = 0.1$, $\tilde{p} = 0.3$, $m_0 = 2$, $\tilde{q} = 0.02$, $\alpha_u = 0.1$, $\alpha_w = 0.3$, $d_v = 0.2$, $\xi = 0.2$; and the initial point is $[u_1(0), u_2(0), w_1(0), w_2(0), v_1(0), v_2(0)] = [5, 5, 5, 5, 5, 5]$ (color figure online)

References

Abrams PA (1986) Adaptive responses of predators to prey and prey to predators: the failure of the arms-race analogy. Evolution 40(6):1229–1247

Abrams PA (1990) The evolution of anti-predator traits in prey in response to evolutionary change in predators. Oikos 59:147–156

Brown JS, Laundre JW, Gurung M (1998) The ecology of fear: optimal foraging, game theory, and trophic interactions. J Mammal 80:385–399

Chepyzhov VV, Vishik MI (2002) Attractors for equations of mathematical physics. American Mathematical Society, Providence

Cresswell W (2008) Non-lethal effects of predation in bird. Ibis 150:3–17

Day T, Burns JG (2003) A consideration of patterns of virulence arising from host-parasite coevolution. Evolution 57(3):671–676

De Leenheer P, Mohapatra A, Ohms HA, Lytle DA, Cushing JM (2017) The puzzle of partial migration: adaptive dynamics and evolutionary game theory perspectives. J Theor Biol 412:172–185

Diekmann O (2004) A beginner's guide to adaptive dynamics. Banach Center Publ 63:47–86

Geritz SAH, Kisdi E, Meszena G, Metz JAJ (1998) Evolutionary singular strategies and the adaptive growth and branching of evolutionary tree. Evol Ecol 12:35–57

Hastings A (1982) Dynamics of a single species in a spatially varying environment: the stabilizing role of high dispersal rates. J Math Biol 16:49–55

Hastings A (1983) Can spatial variation along lead to selection for dispersal? Theor Popul Dyn 24:244–251

Jansen VAA (2001) The dynamics of two diffusively coupled predator–prey populations. Theor Popul Biol 59:119–131

Křivan V (2007) The Lotka–Volterra predator–prey model with foraging-predation risk trade-offs. Am Nat 170(5):771–782

Levin SA, Cohen D, Hastings A (1984) Dispersal strategies in patchy environments. Theor Popul Biol 26:165–191

Lima SL, Dill LM (1990) Behavioral decisions made under the risk of predation: a review and prospectus. Can J Zool 68:619–640

Lundberg P (2013) On the evolutionary stability of partial migration. J Theor Biol 321:36–39

Nelson EH, Matthews CE, Rosenheim JA (2004) Predators reduce prey population growth by inducing changes in prey behavior. Ecology 85:1853–1858

Okubo A, Levin SA (2001) Diffusion and ecological problems: modern perspectives. Springer, New York

Preisser EL, Bolnick DI, Benard MF (2005) Scared To death? The effects of intimidation and consumption in predator–prey interactions. Ecology 86:501–509

Rosenzweig ML, MacArthur RH (1963) Graphical representation and stability conditions of predator–prey interactions. Am Nat 97:209–223

Sasmal SK (2018) Population dynamics with multiple Allee effects induced by fear factors a mathematical study on prey–predator interactions. Appl Math Model 64:1–14

Sasmal SK, Takeuchi Y (2020) Dynamics of a predator–prey system with fear and group defense. J Math Anal Appl 481:12347

Takeuchi Y, Wang W, Nakaoka S, Iwami S (2009) Dynamical adaptation of parental care. Bull Math Biol 71:931–951

Terry AJ (2015) Predator–prey models with component Allee effect for predator reproduction. J Math Biol 71:1325–1352

Wang X, Zou X (2017) Modeling the fear effect in predator–prey interactions with adaptive avoidance of predators. Bull Math Biol 79:1325–1359

Wang X, Zou X (2018) Pattern formation of a predator–prey model with the cost of anti-predator behaviors. Math Biosci Eng 15:775–805

Wang Y, Zou X (2020) On a predator–prey system with digestion delay and anti-predation strategy. J Nonlinear Sci 30:1579–1605

Wang X, Zanette LY, Zou X (2016) Modelling the fear effect in predator–prey interactions. J Math Biol 73:1179–1204

Zanette LY, White AF, Allen MC, Clinchy M (2011) Perceived predation risk reduces the number of offspring songbirds produce per year. Science 334:1398–1401

Zu J, Takeuchi Y (2012) Adaptive evolution of anti-predator ability promotes the diversity of prey species: critical function analysis. BioSystems 109:192–202

Publisher's Note Springer Nature remains neutral with regard to jurisdictional claims in published maps and institutional affiliations.